Crystal fields, exchange, and conduction electron polarization in $SmAl_2$

A. Barla,[1,2,*] J. P. Sanchez,[1] F. Givord,[1,†] J. X. Boucherle,[1,†] B. P. Doyle,[2,3] and R. Rüffer[2]
[1]*Département de Recherche Fondamentale sur la Matière Condensée, CEA Grenoble, 17 rue des Martyrs, F-38054 Grenoble Cedex 9, France*
[2]*European Synchrotron Radiation Facility, BP 220, F-38043 Grenoble Cedex 9, France*
[3]*Laboratorio TASC-INFM, Area Science Park, Basovizza S.S. 14 Km 163.5, I-34012 Trieste, Italy*
(Received 4 October 2004; published 19 January 2005)

We have applied ^{149}Sm nuclear forward scattering of synchrotron radiation to study the properties of the Sm sublattice in $SmAl_2$. A self-consistent analysis of the neutron magnetic form factor together with the thermal variation of the ^{149}Sm hyperfine interaction parameters and of the bulk magnetization was carried out. This enabled us to refine the crystal field and exchange parameters and to deduce the temperature dependence of the $4f$ magnetic moment and of the conduction electron polarization.

DOI: 10.1103/PhysRevB.71.012407 PACS number(s): 75.10.Dg, 75.30.Cr, 76.80.+y, 71.70.Ch

Among the trivalent rare-earth ions, Sm^{3+} exhibits unique magnetic properties which arise from the interplay between the J-mixing effects for the $4f$ multiplets and the near cancellation of the orbital and spin $4f$ magnetic moments.[1] Indeed, it is known that the Sm^{3+} ion has a small gap ($\sim$1500 K) between the ground ($^6H_{5/2}$) and first excited ($^6H_{7/2}$) multiplets. Therefore J is no longer a good quantum number and one has to consider relatively large matrix elements between the consecutive multiplets, which influences considerably the magnetic properties. The other specificity of the Sm^{3+} ion's ground multiplet is its small Landé factor ($g_J=2/7$) and in turn the similar sizes for the spin (μ_S) and orbital (μ_L) parts of the localized $4f$ moments which, owing to the spin-orbit interaction, couple antiparallel. This leads to a resulting low $4f$ moment ($0.71\mu_B$ for the free Sm^{3+} ion). When the Sm^{3+} ion is embedded in a solid the crystal field and the exchange interactions further modify its magnetic behavior and in metallic systems, the conduction electron polarization may play a crucial role.[2]

Due to the peculiarities mentioned above, the magnetism of samarium and its compounds has attracted considerable interest despite some difficulties encountered in the analysis of the experimental data.[3–6] During the last decades special attention was paid to the study of the effects of crystal fields, exchange, and conduction electron polarization on the properties of Sm materials. An important breakthrough was provided by neutron magnetic form factor measurements which enabled one not only to evaluate the $4f$ moment but also to deduce values for the exchange and crystal field parameters and to determine the ground-state wave function.[7] Moreover, comparison with bulk magnetization data allowed one to estimate the conduction electron polarization (μ_{ce}) in ferromagnets. Such types of investigations clearly demonstrated that μ_{ce} parallel to the $4f$ spin moment could be of the same magnitude as the total moment. More recently, Adachi *et al.* obtained similar information by analyzing the temperature dependence of the ordered moment of various Sm ferromagnets such as hcp Sm (Ref. 8) and cubic $SmAl_2$, SmZn, and SmCd (Ref. 9). It has also been shown that the magnitude and even the sign of the $4f$-induced Sm magnetic hyperfine field could be strongly affected by crystal field effects.[5] Thus, special care should be taken to interpret hyperfine field data obtained either by NMR (Ref. 10) or the Mössbauer effect (Ref. 11). However, the most dramatic example of the peculiar properties of Sm-based compounds was the discovery of a ferromagnet having no net magnetic moment.[12] This was nicely demonstrated by magnetic Compton scattering[13] and nonresonant ferromagnetic x-ray diffraction[14] of synchrotron radiation on $Sm_{1-x}Gd_xAl_2$ samples. It was shown that at the compensation temperature ($T_{comp}\sim 84$ K for $x=0.018$) the spin and orbital moments exactly cancel ($\mu_S=\mu_L$) while, below T_{comp}, $\mu_L>\mu_S$ whereas, above T_{comp}, $\mu_S>\mu_L$. Such a result implies that the compensation mechanism is driven by different temperature dependences of the $4f$ spin and orbital moments due to the multiplet admixture arising from crystal field and exchange interactions. Note that, in the absence of J-mixing effects, as observed for example in the heavy rare earths, μ_L and μ_S have the same temperature dependence and according to the Wigner-Eckart theorem the ratio μ_L/μ_S is constant at any temperature.

In this article, we report on the temperature dependences of the ^{149}Sm hyperfine magnetic field and quadrupole coupling constant in undoped $SmAl_2$ obtained by performing ^{149}Sm nuclear forward scattering (NFS) of synchrotron radiation.[15] The hyperfine interaction parameters have been analyzed self-consistently with the neutron magnetic form factor taken from Ref. 7 and with the macroscopic magnetization data taken from Ref. 9 by using a model Hamiltonian whose diagonalization gives the eigenvalues and eigenvectors of the Sm^{3+} ion. This procedure enabled us to refine the crystal field and exchange parameters and to deduce the temperature dependence of the $4f$ magnetic moment and of the conduction electron polarization.

$SmAl_2$ is a cubic Laves phase which orders ferromagnetically at $T_C=122$ K with the easy magnetization along the [111] axis. The Sm form factor data obtained at 4.2 K with a field of 1.65 T applied along the easy direction of the single crystal were taken from Ref. 7. The temperature dependence of the macroscopic magnetization used in this work is the one published by Adachi *et al.*[9] The ^{149}Sm NFS measurements (resonant energy $E_0=22.494$ keV, 5/2-7/2 transition) were performed at the undulator beamline ID18 (Ref. 16) of

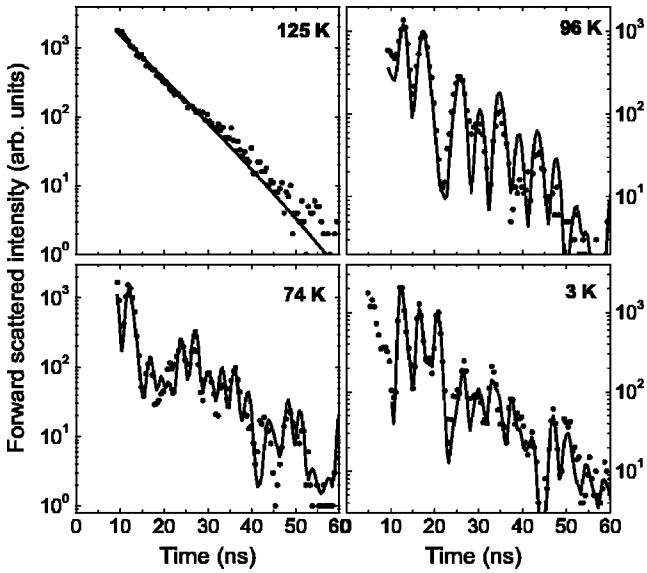

FIG. 1. Selected ^{149}Sm NFS spectra of $SmAl_2$ as a function of temperature above and below T_C. The dots represent experimental data points, while the lines are fits.

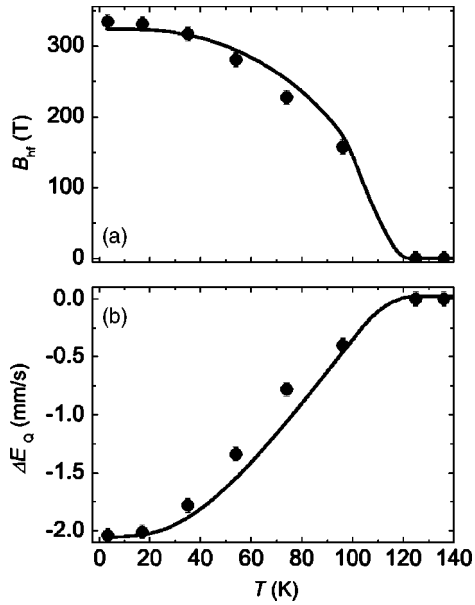

FIG. 2. Temperature dependence of (a) the magnetic hyperfine field B_{hf} and (b) the electric quadrupole interaction ΔE_Q of $SmAl_2$. The solid circles are experimental data points while the lines are fits to them (see text).

the European Synchrotron Radiation Facility (ESRF), Grenoble, France, using a powder sample. The energy bandwidth of the undulator radiation was reduced in two steps to $\Delta E \approx 0.9$ meV. The sample was mounted in a liquid-helium cryostat system allowing for measurements in the temperature range between 3 and 300 K. The scattered radiation was measured by using four stacked avalanche photodiodes.

Figure 1 shows some selected ^{149}Sm NFS spectra collected from 3 K up to 125 K. As shown in the figure, at 125 K (T_C=122 K) one observes a spectrum characteristic of unsplit nuclear levels; i.e., quadrupole or magnetic interactions are absent. The Sm ions are thus, as expected, in the paramagnetic state and in a cubic symmetry. For temperatures below T_C the spectral shape changes significantly and shows clear quantum beats indicating that the nuclear levels are now split by hyperfine interactions. The data analysis was performed with the package MOTIF (Refs. 17,18) by using the full dynamical theory of nuclear resonance scattering including the diagonalization of the complete hyperfine Hamiltonian. The magnetic hyperfine field B_{hf} and the induced quadrupole interaction $\Delta E_Q = eV_{zz}Q$ (Q is the quadrupole moment of the nuclear ground state) were deduced assuming that V_{zz}, the principal component of the electric field gradient, and B_{hf} are parallel. The best fit to the data is obtained with a single set of hyperfine parameters assuming short relaxation times.

The temperature dependences of B_{hf} and ΔE_Q in the whole explored range are shown in Fig. 2. In the magnetically ordered state, the Sm ions feel combined magnetic and quadrupole interactions with saturation values B_{hf} =335(10) T and ΔE_Q=−2.03(6) mm/s [or −36.8(1) MHz], in good agreement with ^{149}Sm NMR data[19] and close to the free ion value of Sm^{3+} [342(10) T and −2.16(10) mm/s; see Ref. 20]. The hyperfine field arises essentially from the $4f$ electrons, which contribute directly through an orbital and spin-dipolar term (B_{4f}) and indirectly via the core polarization (B_{cp}) (B_{4f} and B_{cp} were evaluated by Bleaney[20] to amount, respectively, to 324 and 18 T for the free Sm^{3+} ion). Another contribution, far less important, is due to the polarization of the conduction electrons (B_{ce}) by the Sm $4f$ moments. It could be estimated to amount at most to ∼−7.5 T in $SmAl_2$ by scaling the hyperfine field of −16.2 T measured at the ^{155}Gd nuclei in the parent S-state ion compound $GdAl_2$ (Refs. 21,22). In the following, to simplify, we will assume that the temperature dependence of B_{hf} is described by the orbital and spin-dipolar term which is the leading contribution to B_{hf}.

Like the $4f$ moment or the neutron magnetic form factor,[7] B_{hf} and ΔE_Q are key parameters to characterize the properties of the magnetically ordered state because they are directly related to the eigenfunctions of the thermally populated electronic levels. In the case of Sm^{3+} ions, contributions arising from the mixing of the ground multiplet ($^6H_{5/2}$) with excited states ($^6H_{7/2}$, etc.) are generally involved. To calculate the physical variables like B_{hf} or ΔE_Q it is necessary to obtain the wave functions and the energies of the different levels by diagonalizing the following Hamiltonian:

$$\mathcal{H} = \lambda \mathbf{L} \cdot \mathbf{S} + \mathcal{H}_{CF} - 2J_{ff}\langle \mathbf{S} \rangle \mathbf{S} + \mu_B \mathbf{H}(\mathbf{L} + 2\mathbf{S}), \qquad (1)$$

where $\mathbf{L}$ and $\mathbf{S}$ are, respectively, the orbital and spin angular moment operators. λ is the spin-orbit interaction coefficient taken as 410 K. $\mathcal{H}_{CF} = \Sigma_{k,q} N_k^q B_k^q \mathcal{U}_k^q$ is the crystal field Hamiltonian. The N_k^q and $\mathcal{U}_k^q$ terms are tabulated in Refs. 23 and 24, μ_B is the Bohr magneton and $\mathbf{H}$ is the external field. The free parameters in the calculations are the interionic exchange J_{ff} and the crystal field parameters B_k^q. For cubic symmetry, the second-order contribution B_2^0 is zero and the fourth- and sixth-order terms are restricted to two parameters B_4 and B_6.

TABLE I. Reduced matrix elements related to the hyperfine field and the electric field gradient operators for the Sm^{3+} ion (Refs. 28–30).

$\langle 5/2\|N\|5/2\rangle$	$\langle 7/2\|N\|7/2\rangle$	$\langle 7/2\|N\|5/2\rangle$
1.54921	1.07005	−0.37993
$\langle 5/2\|\alpha\|5/2\rangle$	$\langle 7/2\|\alpha\|7/2\rangle$	$\langle 7/2\|\alpha\|5/2\rangle$
0.04127	0.01934	−0.05023

From the eigenfunctions $|\Psi_i\rangle$ and the energy eigenvalues E_i obtained by diagonalizing the Hamiltonian given by Eq. (1), the hyperfine field (or $4f$ moment) and the quadrupole interaction are calculated from a thermal average of the corresponding operators. For a sublevel i defined by the wave function $|\Psi_i\rangle, B_{\rm hf}^i$ is given by the expression[25]

$$B_{\rm hf}^i = 2\mu_B\langle r^{-3}\rangle\langle\Psi_i|\mathbf{B}_{{\rm op},z}|\Psi_i\rangle, \tag{2}$$

and as the relaxation times for transitions between the levels populated at a temperature T are short relative to the reciprocal of the nuclear Larmor frequencies, the hyperfine field at the temperature T is

$$B_{\rm hf}(T) = \frac{\sum_i B_{\rm hf}^i \exp\left(\frac{-E_i}{kT}\right)}{\sum_i \exp\left(\frac{-E_i}{kT}\right)}. \tag{3}$$

The hyperfine field operator $\mathbf{B}_{{\rm op},z}$ is defined by

$$\langle J,M|\mathbf{B}_{{\rm op},z}|J,M\rangle = M\langle J\|N\|J\rangle,$$

$$\langle J+1,M|\mathbf{B}_{{\rm op},z}|J,M\rangle = \sqrt{(J+1)^2 - M^2}\langle J+1\|N\|J\rangle. \tag{4}$$

Here it is sufficient to consider the mixing of the ground state ($J=5/2$, M) with only the first excited state ($J+1=7/2$, M). $\langle r^{-3}\rangle$ is the expectation value of the inverse cube radius of the $4f$ electron orbital. The $\langle J'\|N\|J\rangle$ reduced matrix elements for the Sm^{3+} ion are given in Table I. For the free Sm^{3+} ion $J=M=5/2$, thus $B_{\rm hf}(\text{free ion}) = 2\mu_B\langle r^{-3}\rangle\{3.87302\} = 342$ T. In a similar way the quadrupole interaction associated with the sublevel $|\Psi_i\rangle$ is given by the expression[25]

$$\Delta E_Q^i = -e^2Q\langle r^{-3}\rangle(1-R)\langle\Psi_i|\mathbf{q}_{{\rm op},z}|\Psi_i\rangle, \tag{5}$$

where $\mathbf{q}_{{\rm op},z}$ is the electric field gradient operator defined by

$$\langle J,M|\mathbf{q}_{{\rm op},z}|J,M\rangle = [3M^2 - J(J+1)]\langle J\|\alpha\|J\rangle,$$

$$\langle J+1,M|\mathbf{q}_{{\rm op},z}|J,M\rangle = M\sqrt{(J+1)^2 - M^2}\langle J+1\|\alpha\|J\rangle. \tag{6}$$

R is the Sternheimer ionic shielding factor and Q the quadrupole moment of the nucleus. The numerical factors $\langle J'\|\alpha\|J\rangle$ are reported in Table I. For the free Sm^{3+} ion one thus obtains $\Delta E_Q(\text{free ion}) = -e^2Q\langle r^{-3}\rangle(1-R)\{0.41270\} = -2.16$ mm/s.

There were many attempts to determine the exchange (J_{ff}) and crystal field (B_4, B_6) parameters of $SmAl_2$ from the analysis of various sets of experimental data including the magnetic susceptibility, Al Knight shift, or neutron magnetic form factor.[7] However, none of them provided precise values of exchange and crystal field parameters. They only led to a possible range of values. A further step was made by Adachi *et al.*[9] who used an extended form of Eq. (1) (they added a term which stands for the conduction electron polarization which was assumed to be proportional to the spin moment) for the analysis of the temperature dependence of the bulk magnetization of a $SmAl_2$ single crystal. Their method allowed the separation of the $4f$ orbital, $4f$ spin and conduction electron contributions to the total ordered moment $\mu_{\rm tot}$ and to restrict the range of possible J_{ff}, B_4, and B_6 values. Although J_{ff} seems to be well defined ($J_{ff} \approx 36$ K), there is still some ambiguity in determining the set of crystal field parameters. B_4 ranges from 50 to 200 K while B_6 appears to be abnormally large ($B_6 \approx 100-140$ K).

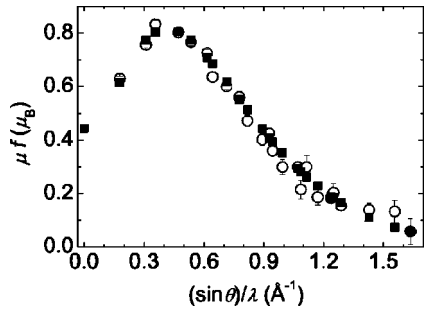

FIG. 3. Comparison of the experimental (open circles), from Ref. 7, and calculated (solid squares) magnetic form factor.

In our work an extended version of a program developed by some of us[24] and based on the Hamiltonian of Eq. (1) was used to fit with the least-squares method the magnetic form factor, the hyperfine field, the quadrupole interaction and the bulk moment $\mu_{\rm tot}$ by taking into account the excited multiplets of the Sm^{3+} ion (see Figs. 2–4). The same model was used to compute the temperature dependence of the $4f$ moment $\mu(T)$ and to evaluate the conduction electron polarization $\mu_{\rm ce}(T) = \mu_{\rm tot}(T) - \mu(T)$ from the fit of the magnetization data obtained by Adachi *et al.*[9] In Fig. 4, the dotted line, which represents the calculated $\mu_{\rm ce}(T)$, assuming that $\mu_{\rm ce} = K\mu_S$ with $K=0.050$, agrees well with the values (open squares) obtained from $\mu_{\rm tot}(T) - \mu(T)$. This demonstrates fur-

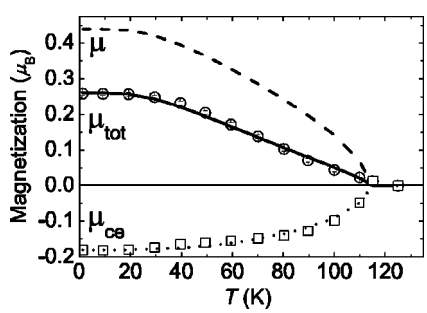

FIG. 4. Thermal variation of the measured macroscopic magnetization $\mu_{\rm tot}$ (open circles) (Ref. 9), of the calculated $4f$ moment μ (dashed line) and of the conduction electron polarization $\mu_{\rm ce}$ (open squares). The solid line is the calculated $\mu_{\rm tot}$ (see text) while the dotted line represents $\mu_{\rm ce}$ calculated assuming that $\mu_{\rm ce} = K\mu_S$ where μ_S is the $4f$ spin moment and $K=0.050$.

ther the validity of our approach. The ground-state wave function obtained from the comparison of the experimental data with our theoretical model is given by

$$\Psi_0 = 0.9593|5/2,-5/2\rangle + 0.2373|5/2,1/2\rangle + 0.0663|7/2,-5/2\rangle + 0.0975|7/2,1/2\rangle - 0.0976|7/2,7/2\rangle. \quad (7)$$

It leads to a saturation Sm moment of $0.44\mu_B$ whose orbital (μ_L) and spin (μ_S) contributions amount to $4.04\mu_B$ and $-3.60\mu_B$, respectively. Note that the ratio $-\mu_L/\mu_S$ is slightly reduced as compared to the Sm^{3+} free ion value (1.20) owing to the mixing effect. The saturated value of the conduction electron polarization is estimated to be $-0.18\mu_B$ while the total moment amounts to $0.26\mu_B$. The free parameters of the Hamiltonian described by Eq. (1) which fit best the data are the following: $J_{ff}=33.3(3)$ K, $B_4=49(4)$ K, and $B_6=-104(5)$ K. The corresponding crystal field coefficients A_4 and A_6, defined as $A_n=B_n/\langle r^n\rangle$, where $\langle r^n\rangle$ are the relativistic free ion radial integrals,[26] are thus estimated to amount to $22(3)\mathrm{Ka}_0^{-4}$ and $-9.9(6)\mathrm{Ka}_0^{-6}$, respectively. It is worth stressing that, without including the quadrupole interaction data to our self-consistent fitting procedure, the sign of A_6 would be undetermined (note that Adachi *et al.*[9] considered only positive A_6 values). The signs of both A_4 and A_6 fit now well with those found along the series of rare-earth $R\mathrm{Al}_2$ compounds.[27] A_6, however, turns out to be about an order of magnitude larger. This latter peculiarity, already noticed by Adachi *et al.*,[9] has not yet received any clear explanation.

In conclusion we have applied ^{149}Sm nuclear forward scattering of synchrotron radiation to determine the temperature dependence of the magnetic hyperfine field and of the electric quadrupole interaction in $SmAl_2$. The self-consistent analysis, based on a model Hamiltonian, of these parameters together with the magnetic form factor from Ref. 7 and the bulk magnetization from Ref. 9 has allowed us to calculate the crystal field and exchange parameters and to deduce the temperature dependence of the $4f$ magnetic moment and of the conduction electron polarization.

J.P.S. is grateful to G. Amoretti and N. Magnani for helpful discussions.

*Now at IPCMS/GEMME, 23 rue du Loess, F-67034 Strasbourg Cedex 2, France.
†CNRS staff.

[1] H. W. de Wijn, A. M. van Diepen, and K. H. J. Buschow, Phys. Status Solidi B **76**, 11 (1976).
[2] A. M. Stewart, Phys. Rev. B **6**, 1985 (1972).
[3] H. W. de Wijn, A. M. van Diepen, and K. H. J. Buschow, Phys. Rev. B **7**, 524 (1973).
[4] K. H. J. Buschow, A. M. van Diepen, and H. W. de Wijn, Phys. Rev. B **8**, 5134 (1973).
[5] S. K. Malik and R. Vijayaraghavan, Phys. Rev. B **12**, 1098 (1975).
[6] S. K. Malik, W. E. Wallace, and R. Vijayaraghavan, Phys. Rev. B **19**, 1671 (1979).
[7] J. X. Boucherle, D. Givord, J. Laforest, J. Schweizer, and F. Tasset, J. Phys. (Paris), Colloq. **40**, C5–180 (1979).
[8] H. Adachi, H. Ino, and H. Miwa, Phys. Rev. B **56**, 349 (1997).
[9] H. Adachi, H. Ino, and H. Miwa, Phys. Rev. B **59**, 11 445 (1999).
[10] R. L. Streever, Phys. Rev. B **12**, 4653 (1975).
[11] I. Nowik and S. Ofer, J. Appl. Phys. **39**, 1252 (1968).
[12] H. Adachi and H. Ino, Nature (London) **401**, 148 (1999).
[13] H. Adachi, H. Kawata, H. Hashimoto, Y. Sato, I. Matsumoto, and Y. Tanaka, Phys. Rev. Lett. **87**, 127202 (2001).
[14] J. W. Taylor, J. A. Duffy, A. M. Bebb, M. R. Lees, L. Bouchenoire, S. D. Brown, and M. J. Cooper, Phys. Rev. B **66**, 161319(R) (2002).
[15] For a detailed description of nuclear forward scattering see, e.g., W. Sturhahn, J. Phys.: Condens. Matter **16**, S497 (2004), and references therein or the web page http://www.esrf.fr/exp_facilities/ID18/pages/technique/index.html
[16] R. Rüffer and A. I. Chumakov, Hyperfine Interact. **97-98**, 589 (1996).
[17] Y. V. Shvyd'ko, Phys. Rev. B **59**, 9132 (1999).
[18] Y. V. Shvyd'ko, Hyperfine Interact. **125**, 173 (2000).
[19] R. Vijayaraghavan, K. Shimizu, J. Itoh, A. K. Grover, and L. C. Gupta, J. Phys. Soc. Jpn. **43**, 1854 (1977).
[20] B. Bleaney, in *Magnetic Properties of Rare Earth Metals*, edited by R. J. Elliott (Plenum Press, New York, 1972), p. 383.
[21] M. A. H. McCausland and I. S. Mackenzie, Adv. Phys. **28**, 305 (1979).
[22] A. Barla, J. P. Sanchez, B. Malaman, B. P. Doyle, and R. Rüffer, Phys. Rev. B **69**, 220405(R) (2004).
[23] M. J. Weber and R. W. Bierig, Phys. Rev. **134**, 1492 (1964).
[24] F. Givord, J.-X. Boucherle, E. Lelièvre-Berna, and P. Lejay, J. Phys.: Condens. Matter **16**, 1211 (2004).
[25] S. Ofer, I. Nowik, and S. Cohen, in *Chemical Applications of Mössbauer Spectroscopy*, edited by V. I. Goldanskii and R. H. Herber (Academic Press, New York, 1968), p. 427.
[26] A. Freeman and J. P. Desclaux, J. Magn. Magn. Mater. **12**, 11 (1979).
[27] O. Moze, in *Handbook of Magnetic Materials*, edited by K. H. J. Buschow (North-Holland, Amsterdam, 1998), Vol. 11, p. 43.
[28] R. J. Elliott and K. W. H. Stevens, Proc. R. Soc. London, Ser. A **218**, 553 (1953).
[29] R. J. Elliott and K. W. H. Stevens, Proc. R. Soc. London, Ser. A **219**, 387 (1953).
[30] N. Magnani and G. Amoretti (private communication).